Impact of Advanced Extravascular Calcified Plaque on the Assessment of Coronary Stenosis Severity

İlerlemiş Ekstravasküler Kalsifiye Plağın Koroner Stenoz Ciddiyetinin Değerlendirilmesine Etkisi

CASE REPORT
OLGU SUNUMU

ABSTRACT

Coronary computed tomography angiography (CCTA) and CT-derived fractional flow reserve (FFR$_{CT}$) provide high diagnostic accuracy for coronary artery disease (CAD), consistent with invasive coronary angiography (ICA), the gold standard diagnostic technique. The presence of calcified components, however, complicates the interpretation of coronary stenosis severity. We present a case where there was a discrepant assessment of coronary stenosis severity between CCTA/FFR$_{CT}$ (indicating significant obstructive CAD) and ICA (showing no apparent obstructive CAD). CCTA/FFR$_{CT}$ revealed that the stenotic lesion, located in the middle segment of the left circumflex artery, was surrounded by plaque components. The proximal and distal portions of the stenotic lesion consisted of 80.9% luminal volume, 0.2% low-attenuation plaque, 13.4% intermediate-attenuation plaque, and 5.5% calcified plaque. In contrast, the stenotic lesion itself contained 50.0% luminal volume, 0.3% low-attenuation plaque, 26.7% intermediate-attenuation plaque, and 22.9% calcified plaque. Invasive coronary angiography showed no apparent obstructive CAD, implying that the lesions appearing as significant obstructive CAD on CCTA/FFR$_{CT}$ were likely overestimated due to the effects of extravascular calcified plaque. Advanced extravascular calcified plaque surrounding the lesion may cause several artifacts (such as blooming and/or beam hardening artifacts) and/or vasodilator dysfunction (either organic and/or functional), potentially leading to an overestimation of the severity of coronary stenosis in CCTA/FFR$_{CT}$ assessments.

Keywords: Calcified plaque, coronary artery disease, coronary computed tomography angiography, fractional flow reserve

ÖZET

Koroner bilgisayarlı tomografi anjiyografi (BT) ve BT kaynaklı fraksiyonel akım rezervi (FFR$_{CT}$), koroner arter hastalığı (KAH) için altın standart tanı tekniği olan invaziv koroner anjiyografi (ICA) ile uyumlu olarak yüksek tanısal doğ/ruluk sağlar. Bununla birlikte, kalsifiye bileşenlerin varlığı koroner darlık şiddetinin yorumlanmasını zorlaştırmaktadır. Bu yazıda, koroner BT anjiyografi/ FFR$_{CT}$ (belirgin obstrüktif KAH olduğunu gösteren) ve ICA (belirgin obstrüktif KAH olmadığını gösteren) arasında koroner stenoz şiddetinin farklı değerlendirildiği bir vaka sunulmuştur. Koroner BT anjiyografi /FFR$_{CT}$, sol sirkumfleks arterin orta segmentinde yer alan stenotik lezyonun plak bileşenleri ile çevrili olduğunu ortaya koymuştur. Stenotik lezyonun proksimal ve distal kısımları %80,9 lüminal hacim, %0,2 düşük atenüasyonlu plak, %13,4 orta atenüasyonlu plak ve %5,5 kalsifiye plaktan oluşuyordu. Buna karşılık, stenotik lezyonun kendisi %50,0 lüminal hacim, %0,3 düşük atenüasyonlu plak, %26,7 orta atenüasyonlu plak ve %22,9 kalsifiye plak içeriyordu. İnvaziv koroner anjiyografide belirgin bir obstrüktif KAH görülmemiştir, bu da koroner BT anjiyografi /FFRCT'de belirgin obstrüktif KAH olarak görünen lezyonların muhtemelen ekstravasküler kalsifiye plağın etkileri nedeniyle olduğundan fazla tahmin edildiğini göstermektedir. Lezyonu çevreleyen gelişmiş ekstravasküler kalsifiye plak çeşitli artefaktlara (parıldama ve/veya ışın sertleşmesi artefaktları gibi) ve/veya vazodilatör disfonksiyona (organik ve/veya fonksiyonel) neden olarak koroner BT anjiyografi/FFRCT'de değerlendirmelerinde koroner stenozun ciddiyetinin olduğundan fazla tahmin edilmesine yol açabilir.

Anahtar Kelimeler: Kalsifiye plak, koroner arter hastalığı, koroner bilgisayarlı tomografi anjiyografi, fraksiyonel akım rezervi

Toshimitsu Tsugu[1] iD
Kaoru Tanaka[1] iD
Mayuko Tsugu[1] iD
Yuji Nagatomo[2] iD
Johan De Mey[1] iD

[1]*Department of Radiology, Universitair Ziekenhuis Brussel, Brussels, Belgium*
[2]*Department of Cardiology, National Defense Medical College Hospital, Tokorozawa, Japan*

**Corresponding author:**
Toshimitsu Tsugu
✉ tsugu917@gmail.com

Non-invasive assessment tools, such as coronary computed tomography angiography (CCTA) and CT-derived fractional flow reserve (FFR$_{CT}$), provide high diagnostic accuracy for evaluating coronary stenosis severity, comparable to invasive coronary angiography (ICA). The presence of calcified components, however, complicates the interpretation of coronary stenosis severity. It is a common radiological finding that
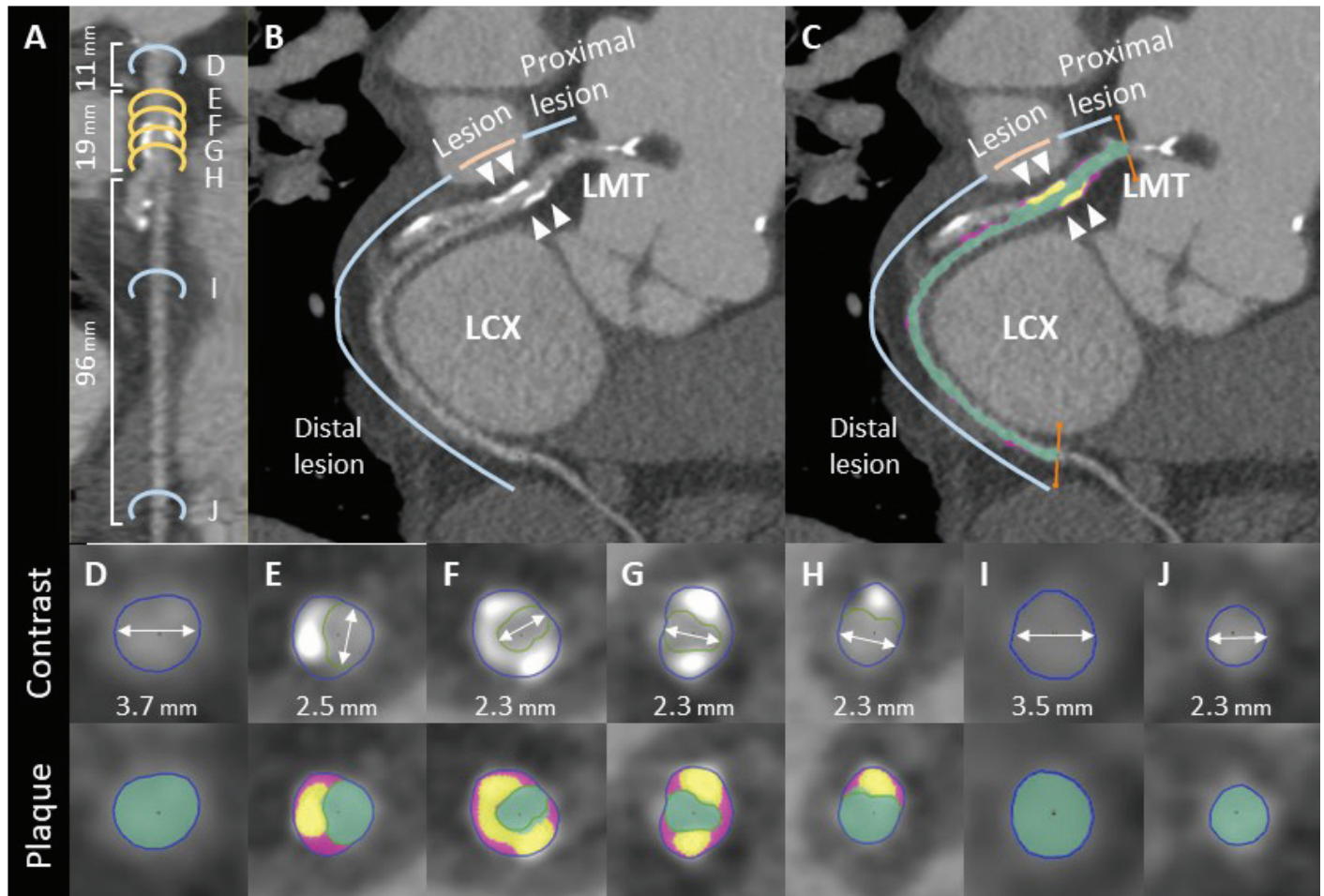
Figure 1. CCTA. (A) Stretched multiplanar reformation of the LCX. (B and C) Curved multiplanar reformation of the LCX. (C and lower panels of D-J) Color-coded plaque image of the LCX. (D-J) Short axis images coinciding with stretched multiplanar reformation. Each axial image corresponds to a stretched multiplanar reformat. Calcified plaque (arrowhead). Color Code Plaque images: Green represents lumen volume, Red indicates intermediate-attenuation plaque, and Yellow denotes calcified plaque. LCX, Left circumflex artery; LMT, Left main trunk.

calcified plaque (CP) causes several artifacts (including blooming and/or beam hardening artifacts) and interferes with accurate CCTA/FFR$_{CT}$ diagnosis. Furthermore, CP may cause heterogeneous vasodilator dysfunction (either organic and/or functional) and generate abrupt changes in luminal diameter between stenotic and peri-stenotic lesions, resulting in energy loss due to turbulent eddies and the overestimation of coronary severity. No reports have specifically focused on CP as the cause of discrepant interpretations of coronary stenosis severity between CCTA/FFR$_{CT}$

ABBREVIATIONS

CAD	Coronary Artery Disease
CCTA	Coronary Computed Tomography Angiography
CP	Calcified Plaque
FFR$_{CT}$	CT-Derived Fractional Flow Reserve
IAP	Intermediate-Attenuation Plaque
ICA	Invasive Coronary Angiography
LAP	Low-Attenuation Plaque
LCX	Left Circumflex Artery
NACAD	No Apparent Coronary Artery Disease
SOCAD	Significant Obstructive Coronary Artery Disease

and ICA. Herein, we present a case of discrepant interpretation of coronary stenosis severity between CCTA/FFR$_{CT}$ (indicating significant obstructive coronary artery disease [SOCAD]) and ICA (showing no apparent coronary artery disease [NACAD]) in a lesion surrounded by advanced extravascular calcified plaque. This case investigates the discrepancy between CCTA/FFR$_{CT}$ and ICA by analyzing the calcified components (low-attenuation plaque, intermediate-attenuation plaque, and CP) of both the stenotic lesion and its proximal and distal portions.

Case Report

A 73-year-old man was referred to our hospital with chest discomfort on exertion. According to the Society of Cardiovascular Computed Tomography guidelines,[1] sublingual nitrate (0.8 mg, two sprays) was administered five minutes before CCTA scanning. CCTA revealed SOCAD (coronary artery disease (CAD) reporting and data system classification:[2] 4A) at the middle segment of the left circumflex artery (LCX). Vessel morphology and components of each segment (the stenotic lesion and its proximal and distal portions) were measured using GE AW server 3.2 software and Colour Code Plaque (General Electric

Healthcare, Chicago, Illinois, USA). Vessel components were characterized based on Hounsfield units (HU): low-attenuation plaque (LAP) (< 30 HU), intermediate-attenuation plaque (IAP) (30-150 HU), and CP (> 150 HU).[3-5] FFR$_{CT}$ (HeartFlow Inc., Redwood City, California, USA) was calculated based on a three-dimensional anatomical model synthesized from CCTA data.[3-8] The vessel lengths of the proximal portion, stenotic lesion, and distal portion were 11 mm, 19 mm, and 96 mm, respectively (Figures 1A-B). The proximal and distal portions contained mild

IAP, whereas the stenotic lesion was characterized by abundant IAP and CP (Figures 1C-J and 2), particularly in the middle part of the stenotic lesion surrounded by CP (Figure 1F). The lumen diameter at the proximal LCX was 3.7 mm, decreasing to 2.3 mm at the maximum stenotic lesion and increasing to 3.5 mm just distal to the stenotic lesion (Figures 1D-J). Peri-stenotic lesions (proximal and distal portions) consisted of 1,011.5 mm³ (80.9%) luminal volume, 2.7 mm³ (0.2%) LAP, 168.0 mm³ (13.4%) IAP, and 68.3 mm³ (5.5%) CP, whereas the stenotic lesion
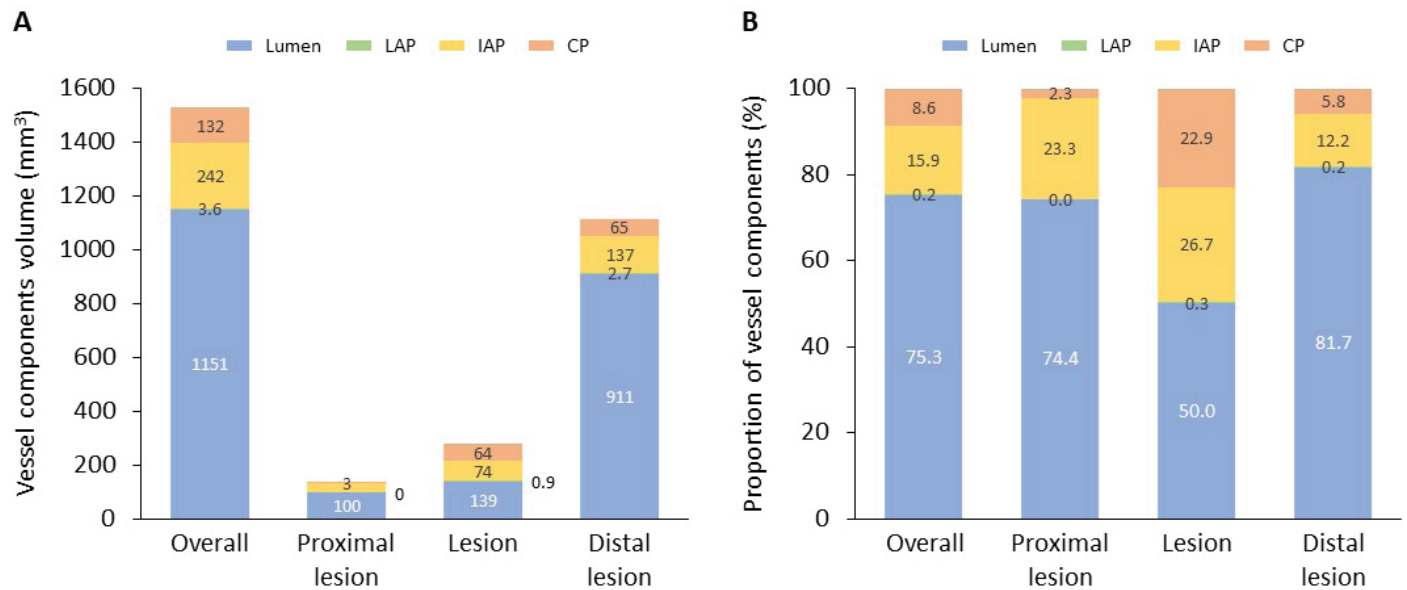
Figure 2. Vessel components at stenotic lesion and its proximal and distal portions: (A) Absolute value of vessel components at each segment. (B) Proportion of vessel components at each segment.
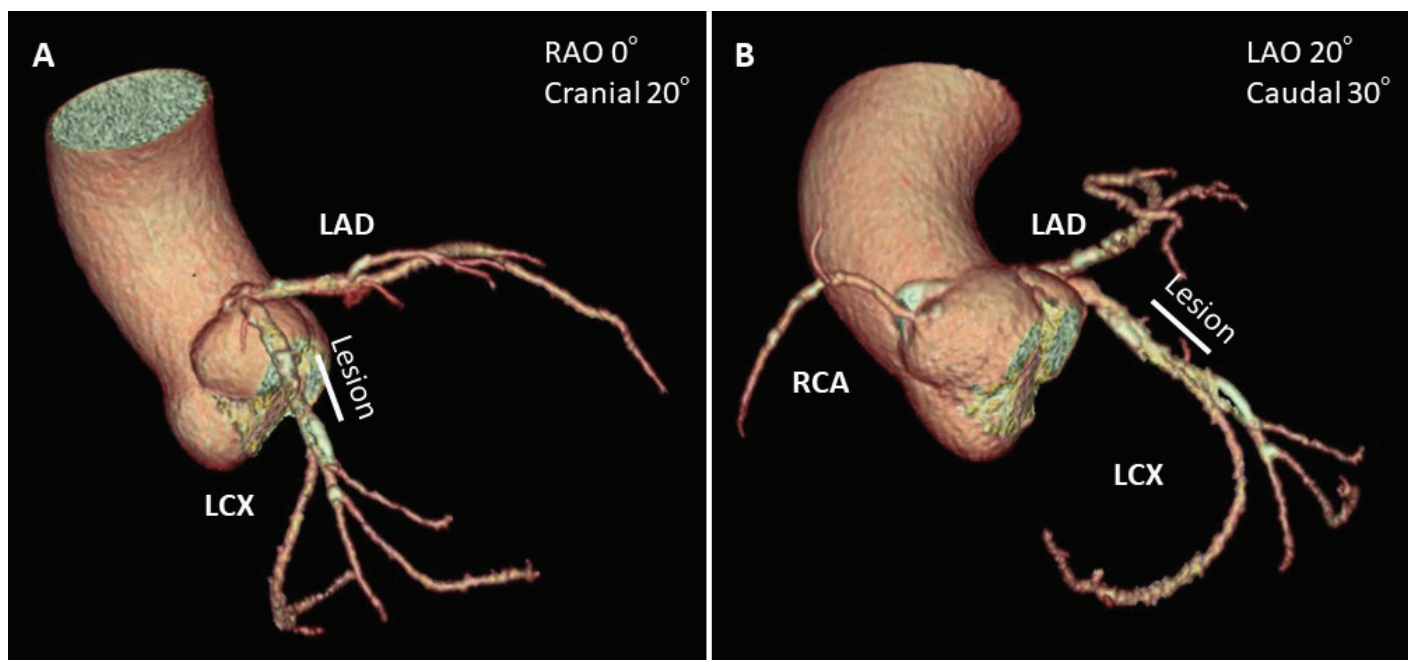
Figure 3. Three-dimensional volume rendered image of the coronary tree. (A) RAO 0°, Cranial 20° view. (B) LAO 20°, Caudal 30° view. LAD, left anterior descending artery; LAO, left anterior oblique; LCX, left circumflex artery; RAO, right anterior oblique; RCA, right coronary artery.

Tsugu et al. Impact of calcified plaques on CCTA/FFR$_{CT}$

Turk Kardiyol Dern Ars 2024;52(4):284–289

consisted of 139.3 mm^3 (50.0%) luminal volume, 0.9 mm^3 (0.3%) LAP, 74.4 mm^3 (26.7%) IAP, and 63.9 mm^3 (22.9%) CP. Notably, although the absolute volume of CP was almost the same, the proportion of CP was significantly larger in the lesion than in peri-lesions (Figures 2A–B). Three-dimensional volume-rendered images of the coronary tree showed that the lesion was located in the middle segment of the LCX, and there

Figure 4. FFR$_{CT}$. (A and B) RAO 30°, Cranial 20° view. (C and D) LAO 20°, Caudal 30° view. (A and C) Overall view. (B and D) Magnified views. Abbreviations are shown in Figure 3.

were no bifurcations or branches from the proximal LCX to the lesion (Figures 3A–B). FFR$_{CT}$ at the proximal portion was 0.99 and dropped to 0.74 at the distal lesion. FFR$_{CT}$ gradually decreased to 0.60 at the end of the LCX (Figures 4A–D). ICA showed no significant coronary artery disease (NSCAD) in the LCX (Figures 5A–B and Videos 1–2), suggesting that the lesion appearing as SOCAD on CCTA/FFR$_{CT}$ was likely overestimated due to the effects of extravascular CP. During the one year following ICA, the patient had an uneventful clinical course and did not develop any cardiovascular symptoms.

Discussion

In the present case, the assessment of coronary stenosis severity was discrepant between CCTA/FFR$_{CT}$ (SOCAD) and ICA (NACAD). This discrepancy may be attributed to an unusual condition of advanced extravascular CP. The presence of extravascular CP significantly impacts the interpretation of CCTA/FFR$_{CT}$ (Supplementary Figure 1). Eccentric intravascular calcified lesions, not scanned in all directions, may lead to inaccurate diagnoses (either underestimation or overestimation) in lesions assessed with ICA. Since our case involved extravascular calcified lesions, it is unlikely to significantly impact the severity of coronary stenosis with ICA.

It is a well-known fact that CP causes several artifacts, including blooming and/or beam hardening, which affect the quality of CCTA images. These artifacts can interfere with an accurate diagnosis of CCTA/FFR$_{CT}$. CT values within a pixel are represented homogeneously, so the presence of calcified components within a pixel increases CT values (due to partial volume effects). As a result, CP appears larger than its actual size and obscures the vessel lumen in the vicinity of CP (blooming artifacts). When the X-ray beam passes through
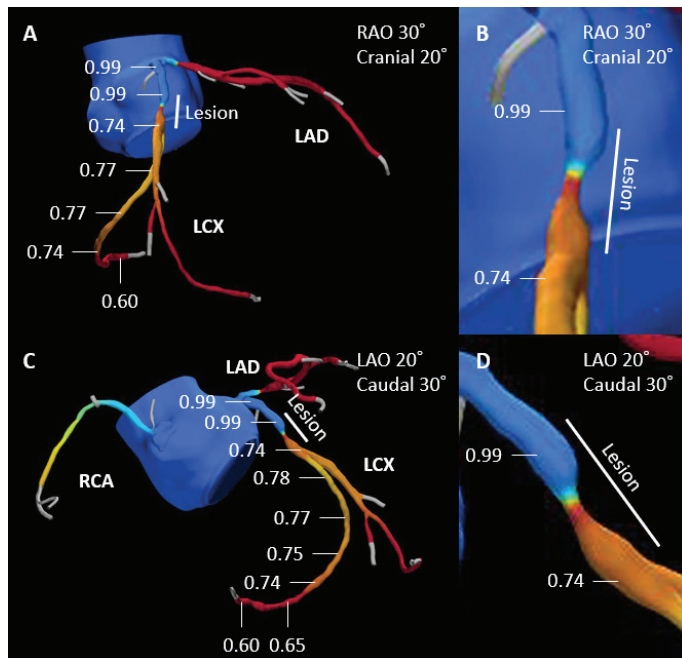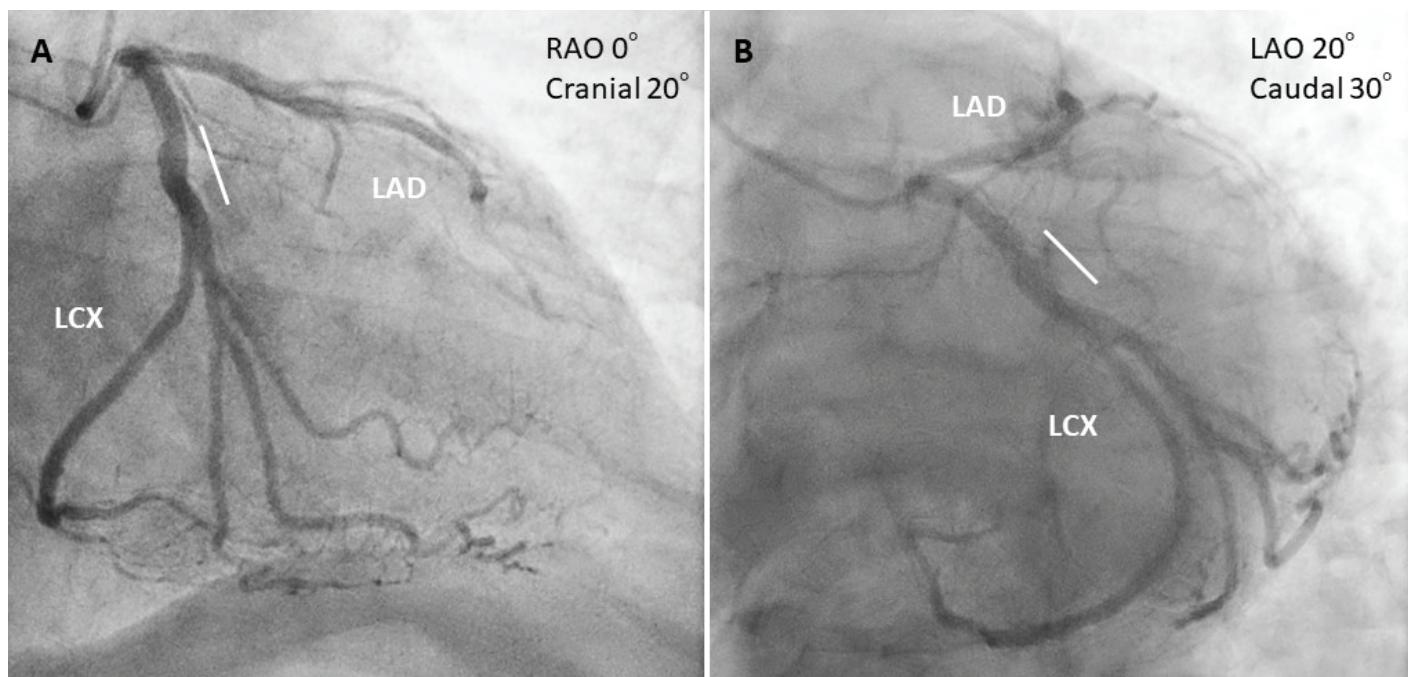
Figure 5. Invasive coronary angiography. (A) RAO 0°, Cranial 20° view. (B) LAO 20°, Caudal 30° view. Lines correspond to lesion sites on CCTA and FFR$_{CT}$. Abbreviations are shown in Figure 3.

Turk Kardiyol Dern Ars 2024;52(4):284-289

Tsugu et al. Impact of calcified plaques on CCTA/FFR$_{CT}$

high-density structures such as CP, most low-energy photons are absorbed, making the vessel lumen adjacent to these high-density structures appear as a low-density area. This occurs because only high-energy beams pass through with minimal absorption (beam hardening artifacts).[9] These artifacts can incorrectly make the vessel lumen appear smaller than its actual size. FFR$_{CT}$, which constructs three-dimensional images based on CCTA images and uses computational fluid dynamics to calculate velocities and pressures in simulated vessels, depends on the quality of CCTA images for its diagnostic accuracy. Consequently, CCTA/FFR$_{CT}$ results should generally align. However, the corrective effects of FFR$_{CT}$ on artifacts have the potential to create discrepancies in the assessments of CCTA and FFR$_{CT}$. In the NXT trial, FFR$_{CT}$ demonstrated improved discrimination of CAD in advanced calcified vessels compared to CCTA, offering diagnostic accuracy twice as high and specificity more than three times greater than CCTA.[10] In the Diagnosis of Ischemia-Causing Stenoses Obtained Via Noninvasive Fractional Flow Reserve Computed Tomography (DISCOVER-FLOW) study, FFR$_{CT}$ maintained higher diagnostic accuracy than CCTA even at lower image quality levels in patients with calcification-related artifacts.[11] The high diagnostic accuracy of FFR$_{CT}$ in the setting of calcified vessels may be attributable to the incorporation of corrections for calcium blooming artifacts in the FFR$_{CT}$ calculation process. In our case, however, the correction for artifacts was ineffective due to the abundant CP, resulting in similar assessments by CCTA and FFR$_{CT}$.

Moreover, advanced calcified components could potentially cause vasodilator dysfunction (both organic and/or functional) and lead to abrupt changes in luminal diameter between stenotic and peri-stenotic lesions, resulting in energy loss due to turbulent eddies and overestimation of coronary severity in FFR$_{CT}$ assessment. Advanced calcified components induce functional vasodilatory dysfunction by generating oxidative stress or inflammation at lesion sites. Consequently, luminal diameter differences between lesions and peri-lesions are increased during maximal hyperemia, affecting CCTA and FFR$_{CT}$ assessment. Hoffmann et al.[9] reported that vasodilator agents-induced changes in lumen diameter (vasodilator function) were heterogeneous in normal coronary arteries (20-40%) and lesioned vessels (5-10%). In our previous study,[8] we observed that different proportions of vessel components between normal vessels and lesions composed of intravascular calcified components led to varying vasodilator functions. This resulted in an overestimation of FFR$_{CT}$ values in lesions. The presence of intravascular CP causes heterogeneous vasodilation function between lesions and peri-lesions, generating turbulent eddies and affecting energy dynamics. These mechanisms cause an unexpected FFR$_{CT}$ decline and may lead to an overestimation of coronary stenosis severity (Supplementary Figure 2).

In the present case, CT/FFR$_{CT}$ assessment was influenced by the following two factors, modified by extravascular CP: (1) pseudo-narrowing of the lumen diameter due to several artifacts, and (2) energy loss due to organic and/or functional vasodilator dysfunction. Several artifacts, a result of advanced extravascular CP, caused pseudo-narrowing of the luminal diameter with CCTA. Furthermore, advanced extravascular CP inhibited vasodilator function both organically and functionally during maximum hyperemia, accentuating the difference in luminal diameter between lesion and peri-lesion areas, and dissipating potential energy into kinetic or thermal energy across the stenotic lesion (Supplementary Figure 2). FFR$_{CT}$ analysis, constructed based on CCTA images, resulted in an overdiagnosis of FFR$_{CT}$ values from 0.99 to 0.74 (Figure 4 and Supplementary Figure 1). Therefore, CCTA/FFR$_{CT}$ presented SOCAD, although ICA showed no obstructive coronary artery disease (NOCAD).

In the present case, an assessment of invasive tests, including invasive Fractional Flow Reserve (FFR) and intravascular imaging, was not performed due to the absence of apparent coronary stenosis with ICA. Previous studies have demonstrated that FFR$_{CT}$ can be an alternative to invasive FFR due to the high concordance between FFR$_{CT}$ and invasive FFR.[12-14] Intravascular imaging can assess not only intravascular morphology but also quantify plaque characteristics and turbulent eddies. Computed Tomography Angiography (CTA) may have the potential to be an alternative technique to intravascular imaging, as the quantification of plaque characteristics assessed by intravascular imaging has shown a high correlation with CTA.[15] Analyzing energy loss by quantifying turbulent eddies in coronary arteries is a very important issue. Attempts to quantify turbulent eddies using guidewire with invasive coronary angiography,[16] Computed Tomography (CT) angiography,[17] and Magnetic Resonance Imaging (MRI)[18] have begun. Further studies are required for morphological and physiological assessment using intravascular imaging.

This is the first report to investigate the cause of disagreement between CCTA/FFR$_{CT}$ and ICA in assessing coronary stenosis severity by analyzing the vessel components. Differences in calcified components between lesions and peri-lesion areas may lead to differences in organic and/or functional diastolic dysfunction and affect hemodynamics. When interpreting advanced extravascular CP with CCTA/FFR$_{CT}$, it should be taken into consideration that CP may have the potential to overestimate the severity of coronary stenosis.

Conclusion

Advanced extravascular CP may have the potential to overestimate the severity of coronary stenosis with CCTA/FFR$_{CT}$, resulting in inconsistencies with ICA findings.

Video 1. Invasive coronary angiography. RAO 0°, Cranial 20° view. Abbreviations are shown in Figure 3.

**Video 2.** Invasive coronary angiography. LAO 20°, Caudal 30° view. Abbreviations are shown in Figure 3.

Tsugu et al. Impact of calcified plaques on CCTA/FFR$_{CT}$

Turk Kardiyol Dern Ars 2024;52(4):284–289

References

1. Abbara S, Blanke P, Maroules CD, et al. SCCT guidelines for the performance and acquisition of coronary computed tomographic angiography: A report of the society of Cardiovascular Computed Tomography Guidelines Committee: Endorsed by the North American Society for Cardiovascular Imaging (NASCI). *J Cardiovasc Comput Tomogr*. 2016;10(6):435–449. [CrossRef]

2. Cury RC, Abbara S, Achenbach S, et al. CAD-RADS(TM) Coronary Artery Disease – Reporting and Data System. An expert consensus document of the Society of Cardiovascular Computed Tomography (SCCT), the American College of Radiology (ACR) and the North American Society for Cardiovascular Imaging (NASCI). Endorsed by the American College of Cardiology. *J Cardiovasc Comput Tomogr*. 2016;10(4):269–281. [CrossRef]

3. Tsugu T, Tanaka K, Belsack D, et al. Impact of vascular morphology and plaque characteristics on computed tomography derived fractional flow reserve in early stage coronary artery disease. *Int J Cardiol*. 2021;343:187–193. [CrossRef]

4. Tsugu T, Tanaka K, Belsack D, et al. Effects of left ventricular mass on computed tomography derived fractional flow reserve in significant obstructive coronary artery disease. *Int J Cardiol*. 2022;355:59–64. [CrossRef]

5. Tsugu T, Tanaka K, Nagatomo Y, et al. Impact of coronary bifurcation angle on computed tomography derived fractional flow reserve in coronary vessels with no apparent coronary artery disease. *Eur Radiol*. 2023;33(2):1277–1285. [CrossRef]

6. Tsugu T, Tanaka K, Nagatomo Y, Belsack D, De Maeseneer M, De Mey J. Paradoxical changes of coronary computed tomography derived fractional flow reserve. *Echocardiography*. 2022;39(2):398–403. [CrossRef]

7. Tsugu T, Tanaka K, Nagatomo Y, et al. Impact of ramus coronary artery on computed tomography derived fractional flow reserve (FFR$_{CT}$) in no apparent coronary artery disease. *Echocardiography*. 2023;40(2):103–112. [CrossRef]

8. Tsugu T, Tanaka K, Nagatomo Y, De Maeseneer M, de Mey J. Paradoxical Computed Tomography–Derived Fractional Flow Reserve Changes Due to Vessel Morphology and Constituents. *Turk Kardiyol Dern Ars*. 2023;51(2):146–150. English. [CrossRef]

9. Hoffmann U, Ferencik M, Cury RC, Pena AJ. Coronary CT angiography. *J Nucl Med*. 2006;47(5):797–806.

10. Nørgaard BL, Leipsic J, Gaur S, et al.; NXT Trial Study Group. Diagnostic performance of noninvasive fractional flow reserve derived from coronary computed tomography angiography in suspected coronary artery disease: the NXT trial (Analysis of Coronary Blood Flow Using CT Angiography: Next Steps). *J Am Coll Cardiol*. 2014;63(12):1145–1155. [CrossRef]

11. Min JK, Koo BK, Erglis A, et al. Effect of image quality on diagnostic accuracy of noninvasive fractional flow reserve: results from the prospective multicenter international DISCOVER-FLOW study. *J Cardiovasc Comput Tomogr*. 2012;6(3):191–199. [CrossRef]

12. Douglas PS, Pontone G, Hlatky MA, et al.; PLATFORM Investigators. Clinical outcomes of fractional flow reserve by computed tomographic angiography–guided diagnostic strategies vs. usual care in patients with suspected coronary artery disease: the prospective longitudinal trial of FFR(CT): outcome and resource impacts study. *Eur Heart J*. 2015;36(47):3359–3367. [CrossRef]

13. Koo BK, Erglis A, Doh JH, et al. Diagnosis of ischemia-causing coronary stenoses by noninvasive fractional flow reserve computed from coronary computed tomographic angiograms. Results from the prospective multicenter DISCOVER-FLOW (Diagnosis of Ischemia-Causing Stenoses Obtained Via Noninvasive Fractional Flow Reserve) study. *J Am Coll Cardiol*. 2011;58(19):1989–1997. [CrossRef]

14. Min JK, Taylor CA, Achenbach S, et al. Noninvasive Fractional Flow Reserve Derived From Coronary CT Angiography: Clinical Data and Scientific Principles. *JACC Cardiovasc Imaging*. 2015;8(10):1209–1222. [CrossRef]

15. Dey D, Schepis T, Marwan M, Slomka PJ, Berman DS, Achenbach S. Automated three-dimensional quantification of noncalcified coronary plaque from coronary CT angiography: comparison with intravascular US. *Radiology*. 2010;257(2):516–522. [CrossRef]

16. Ferrari M, Werner GS, Bahrmann P, Richartz BM, Figulla HR. Turbulent flow as a cause for underestimating coronary flow reserve measured by Doppler guide wire. *Cardiovasc Ultrasound*. 2006;4:14. [CrossRef]

17. Chaichana T, Sun Z, Jewkes J. Computation of hemodynamics in the left coronary artery with variable angulations. *J Biomech*. 2011;44(10):1869–1878. [CrossRef]

18. Ha H, Lantz J, Ziegler M, et al. Estimating the irreversible pressure drop across a stenosis by quantifying turbulence production using 4D Flow MRI. *Sci Rep*. 2017;7:46618. [CrossRef]
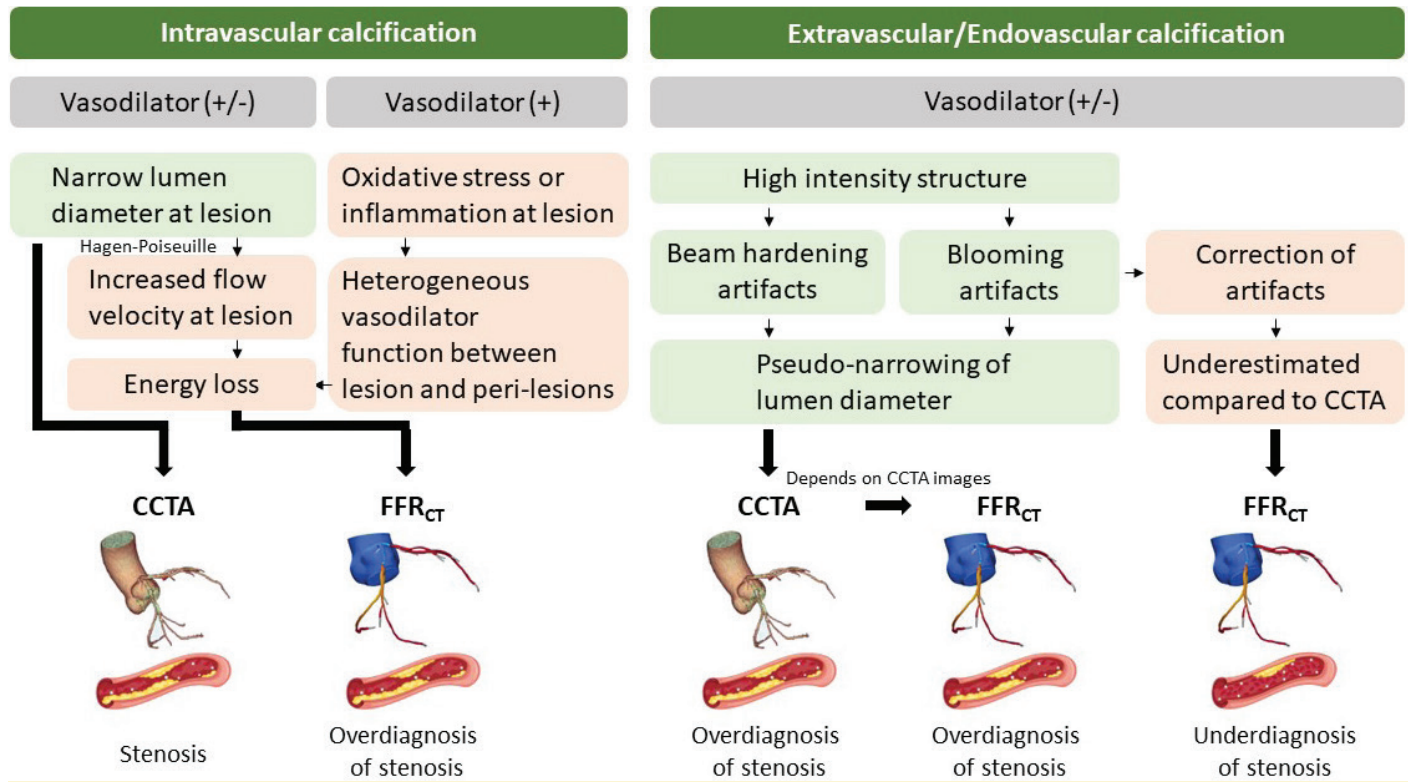
Supplementary Figure 1. Scheme of the effects of extravascular calcification on the assessment of coronary stenosis severity with CCTA and FFR$_{CT}$.
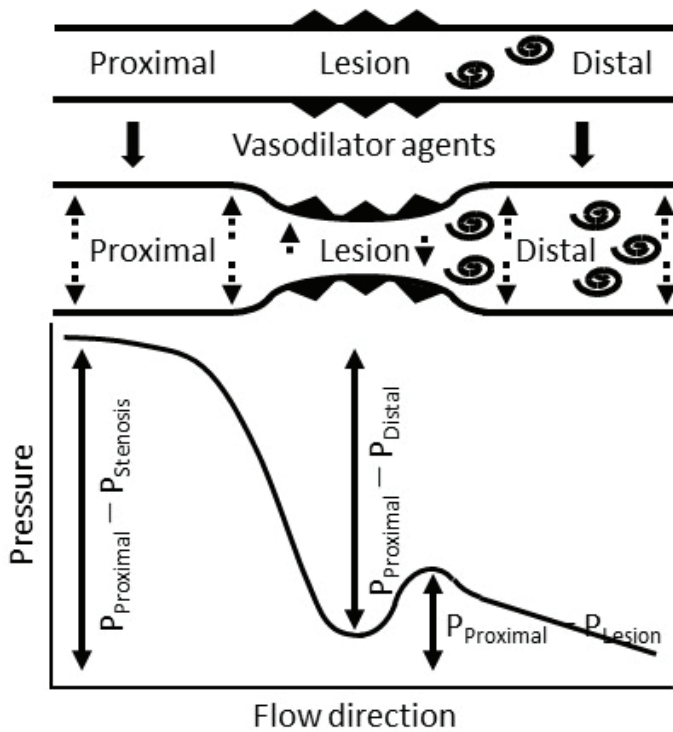
Supplementary Figure 2. Scheme of the impact of organic vasodilator dysfunction on energy hemodynamics.